Improved Partial Cancellation Method for High Frequency Core Loss Measurement

Feiyang Zhu, Qiang Li, Fred C. Lee
Center for Power Electronics Sytems, the Bradley Department of Electrical Engineering
Virginia Polytechnic Institute and State University
Blacksburg, VA 24060, USA

***Abstract*—Accurate high-frequency core loss measurement is critical for power converter design, especially for integrated voltage regulator application. Partial cancellation method is a promising candidate, which can cancel out loss error caused by phase discrepancy without finely tuning cancellation component values. However, it assumes a small value of phase discrepancy, which is not valid for high frequency. This paper performs the error analysis in this case and proposes an initial compensation method to eliminate this error. Finally, experiments are performed to verify proposed method up to 60MHz.**

Keywords – high frequency, core loss measurement, partial cancellation, initial compensation

I. Introduction

With the development of semiconductors like gallium nitride devices, power converters have been pushed to above Megahertz and even higher, especially for integrated voltage regulator application [1]–[7]. Therefore, magnetic design becomes more crucial to achieve higher efficiency and power density, which imposes a challenge for high frequency core loss measurement. The core loss measurement approach can be divided into thermal method and electrical method in general. The basic idea of thermal method [8] is to measure the temperature difference caused by magnetic loss in a thermal chamber. Although accurate, winding loss cannot be excluded and the whole process is time consuming. For the electrical approach, two-winding method is classic in prior arts [9]. By winding the core into a transformer, core loss is measured excluding winding loss. However, this method is sensitive to phase discrepancy caused by sensing resistor parasitic inductance or probe delay time depending on different current sensing methods. For low loss material, a small phase discrepancy will cause huge error.

[10] presented another electrical method utilizing a capacitor in series with the core under test. The capacitor has to be finely tuned to resonate exactly with the magnetizing inductance of the core under testing frequency. Then only equivalent core loss resistor exists and its loss is not sensitive to phase discrepancy. However, the winding loss is included and difficult to estimate accurately. Mu [11] improved this resonant method by combining two-winding method to exclude winding loss. Furthermore, Mu proposed an inductive cancellation method by replacing capacitor with an air core transformer to extend excitation type from sinusoidal excitation to arbitrary excitation. However, the capacitance or mutual inductance value of air core transformer is crucial and a little mismatch from perfect cancellation will cause huge error. Finely tuning capacitor or air core transformer under different testing conditions is time consuming. Hou [12] proposed partial cancellation method to fix this problem, where Figure 1 shows the equivalent circuit. The basic idea of this method is utilizing the loss error in measured air core transformer loss to cancel out loss error in measured core loss. Therefore, it does not require finely tuning cancellation component value. However, it assumes a small value of phase discrepancy when deriving the expressions of loss error of measured air core transformer loss and of measured core loss, which is only valid for low frequency and will introduce extra non-negligible measured core loss error for higher frequency (>5MHz). Therefore, this paper first briefly reviews the working principle of partial cancellation method in section II. In section III, this paper performs the error analysis under high frequency condition, which has not been studied before and then proposes a method to eliminate the induced error by controlling phase discrepancy in a small range. Finally, experiments verify the proposed method in section IV.

II. Working Principle of Partial Cancellation Method

In this section, the working principle of partial cancellation method is briefly reviewed. Figure 1 shows the equivalent circuit. The core voltage v_{core}, air core transformer voltage v_L and current through the core i are measured in this method. Current probe is more stable under different frequencies

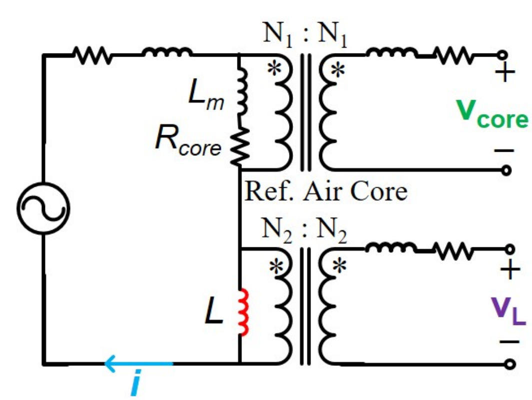

Fig. 1: Equivalent circuit of Hou's inductive partial cancellation method.

among different current sensing methods [13], and is used for measurement and analysis in this paper. Under sinusoidal excitation, the real core loss P_{core} should be

$$P_{core} = V_{core} I cos\varphi \tag{1}$$

Where V_{core} and I are RMS value of v_{core} and i and φ is the real phase angle between v_{core} and i. Due to phase discrepancy $\Delta\varphi$ caused by mismatch of delay time between voltage probe and current probe, the measured core loss has error term ΔP_{core}. By differentiating equation (1) [12] [14], ΔP_{core} is approximated as

$$\Delta P_{core} \approx V_{core} I sin\varphi \Delta\varphi \tag{2}$$

Therefore, the measured core loss P_{core_m} is

$$\begin{aligned} P_{core\_m} &= P_{core} + \Delta P_{core} \\ &\approx V_{core} I cos\varphi + V_{core} I sin\varphi \Delta\varphi \end{aligned} \tag{3}$$

Similarly, the measured air core transformer loss P_{L_m} is

$$P_{L\_m} = 0 + \Delta P_L \approx V_L I \Delta\varphi \tag{4}$$

Since both ΔP_{core} and ΔP_L contain $\Delta\varphi$, ΔP_L is used to cancel out ΔP_{core} to obtain real core loss P_{core}. The ratio of ΔP_L to ΔP_{core} is defined as cancellation factor k_d as shown below,

$$k_d = \frac{\Delta P_L}{\Delta P_{core}} = \frac{V_L}{V_{core} sin\varphi} \tag{5}$$

By combining equation (3)-(5), the real core loss is derived as follow

$$P_{core} = P_{core\_m} - \frac{1}{k_d} P_{L\_m} \tag{6}$$

The value of k_d is difficult to find out directly because of the inaccuracy of measuring φ directly caused by phase discrepancy. A unique method is adding a phase perturbation $\Delta\theta(\sim 1^\circ)$ into current i with the de-skew function of oscilloscope and calculating the value of cancellation factor with measured core loss before and after phase perturbation. The calculated cancellation factor is defined as k_c. k_d is the desired value from math and k_c is the real value applied in the measurement. Therefore, before phase perturbation we have

$$P_{core} = P_{core\_m} - \frac{1}{k_c} P_{L\_m} \tag{7}$$

After phase perturbation, we have

$$P_{core} = P'_{core\_m} - \frac{1}{k_c} P'_{L\_m} \tag{8}$$

$$P'_{core\_m} = V_{core} I cos\varphi + V_{core} I sin\varphi (\Delta\varphi + \Delta\theta) \tag{9}$$

$$P'_{L\_m} = V_L I (\Delta\varphi + \Delta\theta) \tag{10}$$

Combining equation(7) and(8), k_c is calculated as

$$k_c = \frac{P'_{L\_m} - P_{L\_m}}{P'_{core\_m} - P_{core\_m}} = \frac{V_L}{V_{core} sin\varphi} \tag{11}$$

Comparing equation (5) and (11), the value of calculated cancellation factor k_c is exact the same as that of desired cancellation factor k_d. Therefore, we can use k_c to find out real core loss according to equation (7). The nature of insensitive to cancellation component value makes partial cancellation method more promising compared with resonant cancellation methods. However, this method assumes $\Delta\varphi$ as a small value by differentiating P_{core} with respect to φ from equation (1) in the derivation process of expression of ΔP_{core}, which is not valid for high frequency and will introduce extra non-negligible measured core error. This will be analyzed in the next section and an initial compensation method is proposed to eliminate the induced error.

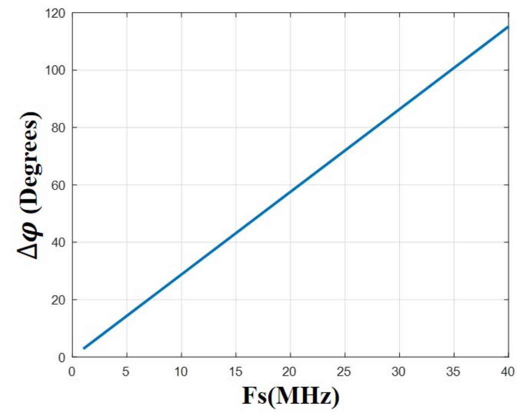

Fig. 2: $\Delta\varphi$ versus frequency with 8ns delay time between voltage probe and current probe.

III. Proposed Improved Partial Cancellation Method

A. Error Analysis of Partial Cancellation Method

First, the extra non-negligible core loss error caused by the assumption of a small value of $\Delta\varphi$ in partial cancellation method is analyzed. The mismatch of probe delay time between voltage probe and current probe will introduce phase discrepancy $\Delta\varphi$ in the measurement system. Take the delay time of voltage probe as a reference,$\Delta\varphi$ is usually a negative value. Therefore, the measured core loss and air core transformer loss under sinusoidal excitation are

$$\begin{aligned} P_{core\_m} &= V_{core} I cos(\varphi - \Delta\varphi) \\ &= V_{core} I cos\varphi + \Delta P_{core\_n} \\ \Delta P_{core\_n} &= V_{core} I [cos\varphi(cos\Delta\varphi - 1) + sin\varphi sin\Delta\varphi] \end{aligned} \tag{12}$$

$$\begin{aligned} P_{L\_m} &= V_L I cos(90^\circ - \Delta\varphi) = 0 + \Delta P_{L\_n} \\ \Delta P_{L\_n} &= V_L I sin\Delta\varphi \end{aligned} \tag{13}$$

In order to analyze the influence of $\Delta\varphi$, the phase discrepancy between current probe TCP0030 and differential voltage probe TDP1000 is taken as an example here. The delay time between TCP0030A and TDP1000 is around 8ns [15] [16], and this equals to different $\Delta\varphi$ under different testing frequencies as shown in Fig 2. For low frequency condition, like 1MHz, $\Delta\varphi \approx 3^\circ$, which is small and we have: cos $\Delta\varphi$-1$\approx$0,sin $\Delta\varphi \approx \Delta\varphi$.Then equation (12) and (13) are simplified to equation (3) and (4). However, $\Delta\varphi$ will be higher than 30°as

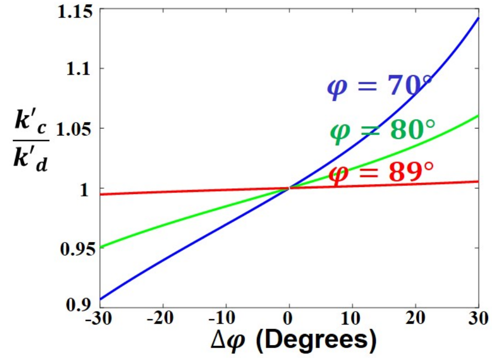

Fig. 3: The impact of $\Delta\varphi$ on the ratio of k'_c to k'_d.

frequency goes above 10MHz and equation (3)-(4) are not accurate any more. In this case, the new defined cancellation factor k'_d is the ratio of ΔP_{core_n} in equation (12) to ΔP_{L_n} in equation (13) as below

$$k'_d = \frac{\Delta P_{L\_n}}{\Delta P_{core\_n}} = \frac{V_L}{V_{core} sin\varphi} \frac{1}{1+\frac{cos\Delta\varphi - 1}{tan\varphi sin\Delta\varphi}} \tag{14}$$

It can be seen that equation (14) simplifies to equation (5) only if $\Delta\varphi$ is small. In order to find out k'_d, a phase perturbation $\Delta\theta(\sim 1°)$ is added into current i with the de-skew function of oscilloscope. Then we have

$$P'_{core\_m} = V_{core} I cos\varphi + V_{core} I [cos\varphi(cos(\Delta\varphi + \Delta\theta) - 1) + sin\varphi sin(\Delta\varphi + \Delta\theta)] \tag{15}$$

$$P'_{L\_m} = V_L I sin(\Delta\varphi + \Delta\theta) \tag{16}$$

Then the new calculated cancellation factor k'_c is

$$k'_c = \frac{P'_{L\_m} - P_{L\_m}}{P'_{core\_m} - P_{core\_m}} = \frac{V_L}{V_{core}} \frac{sina - sin\Delta\varphi}{cos\varphi(cosa - cos\Delta\varphi) + sin\varphi(sina - sin\Delta\varphi)} \tag{17}$$

Where a=($\Delta\varphi$+$\Delta\theta$). Because phase perturbation $\Delta\theta$ is very small, the term sin($\Delta\varphi$+$\Delta\theta$) and cos($\Delta\varphi$+$\Delta\theta$) can be simplified using Taylor series expansion, then equation (17) is simplified as below

$$k'_c \approx= \frac{V_L}{V_{core} sin\varphi} \frac{1}{1 - \frac{tan\Delta\varphi}{tan\varphi}} \tag{18}$$

Comparing equation (14) and (18), the new calculated cancellation factor k'_c is different from the new defined cancellation factor k'_d. The ratio of k'_c and k'_d represents the difference between their values as below

$$\frac{k'_c}{k'_d} = \frac{tan\varphi \sin\Delta\varphi + cos\Delta\varphi - 1}{(tan\varphi - tan\Delta\varphi) sin\Delta\varphi} \tag{19}$$

The smaller the ratio is, the smaller the difference between k'_c and k'_d will be. Fig 3 shows the impact of $\Delta\varphi$ on the ratio under three different cases. Large r$\Delta\varphi$ causes larger difference between k'_c and k'_d. The larger φ is(which means lower loss

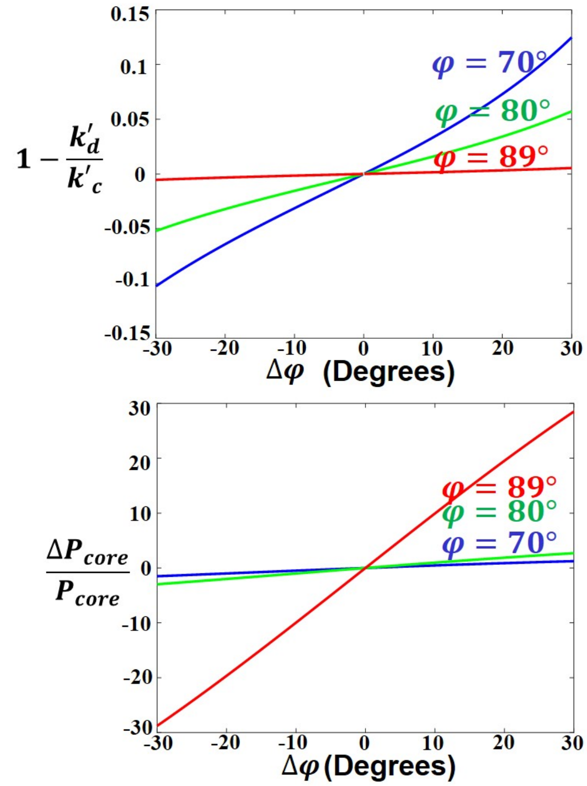

Fig. 4: The impact of $\Delta\varphi$ on the two factors.

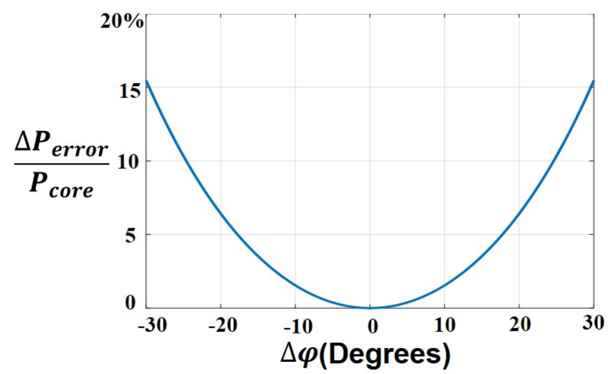

Fig. 5: The impact of $\Delta\varphi$ on the loss error percentage.

material), the smaller the ratio is. Then combining equation (7),(12),(13) and (18), the calculated core loss is

$$P'_{core\_m} - \frac{1}{k'_c} P'_{L\_m} = P_{core} + (1 - \frac{k'_d}{k'_c}) \Delta P_{core\_n} \tag{20}$$

Besides real core loss, another error term exists in equation (20). The loss error percentage is

$$(1 - \frac{k'_d}{k'_c}) \frac{\Delta P_{core\_n}}{P_{core}} = tan\Delta\varphi \sin\Delta\varphi + cos\Delta\varphi - 1 \tag{21}$$

According to equation (21), two factors contribute to the loss error percentage. First is the difference between calculated

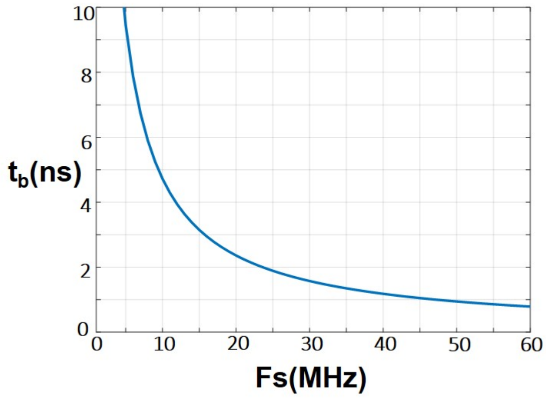

Fig. 6: The tolerable probe delay time vs frequency for <5% loss error percentage.

cancellation factor k'_c and desired cancellation factor k'_d. Another factor is the ratio of measured core loss error ΔP_{core} caused by $\Delta\varphi$ to the real core loss P_{core}. Figure 4 shows the value of these two factors versus $\Delta\varphi$ under three different cases and Figure 5 shows the loss error percentage versus $\Delta\varphi$. It is noteworthy that when φ increases from 70°to 89°, the amplitude of $1\text{-}k'_d/k'_c$ reduces while the ratio of ΔP_{core} to P_{core} increases tremendously. These two factors counterbalance each other and the final loss error percentage is only affected by phase discrepancy $\Delta\varphi$.

Based on equation (21), the loss error exceeds 100% if $\Delta\varphi$ is larger than 60°, which is the case that test frequency is above 20MHz from Fig.2. To limit loss error in a small range, $|\Delta\varphi|$ has to be reduced within a certain value. For example, $|\Delta\varphi|$ need to be controlled less than 17°for less than 5% loss error. By changing 17°into time under different frequency, we can get tolerable probe delay time t_b versus frequency as shown in Fig 6. The delay time between current probe and voltage probe has to be smaller than t_b under interested testing frequency to obtain less than 5% loss error.

B. Proposed Initial Compensation Method

To control delay time between voltage probe and current probe less than t_b, an initial compensation method by using a simple circuit with high Q capacitor is proposed. Fig 7 shows the circuit. By measuring capacitor voltage v_C and its current i under sinusoidal excitation, the high Q capacitor loss P_{C_m} is obtained by integrating the product of v_C and i in a cycle as below

$$P_{C\_m} = P_{ESR} + V_C I sin\Delta\varphi \tag{22}$$

Besides ESR loss P_{ESR}, a large portion of P_{C_m} is caused by $\Delta\varphi$. By excluding P_{ESR} with measured ESR value from impedance analyzer, we can find out $\Delta\varphi$ and corresponding measured probe delay time t_{delay_m} under testing frequency,

$$t_{delay\_m} = \frac{arcsin(\frac{P_{C\_m} - P_{ESR}}{V_C I})}{2\pi f_s} \tag{23}$$

Where f_s is the testing frequency. Then $-t_{delay\_m}$ is added into current probe to initially compensate delay time between voltage probe and current probe by de-skew function of the oscilloscope. After initial compensation, $\Delta\varphi$ is reduced to a value near zero. Then the loss error caused by the rest of $\Delta\varphi$ can be eliminated by partial cancellation method. Fig 8 shows measured probe delay time between current probe TCP0030 and differential voltage probe TDP1000 under different frequency using a 200pF mica high Q capacitor. It can be seen t_{delay_m} changes with testing frequency, which is consistent with the conclusion in [17]. When f_s is higher than 40MHz, t_{delay_m} is larger than 10ns. From Fig 6, the tolerable probe delay time with 5% loss error should be less than 1ns when f_s is higher than 40MHz. Therefore, the fixed 8ns delay time from datasheet [15] [16] cannot be used for initial compensation for higher frequency.

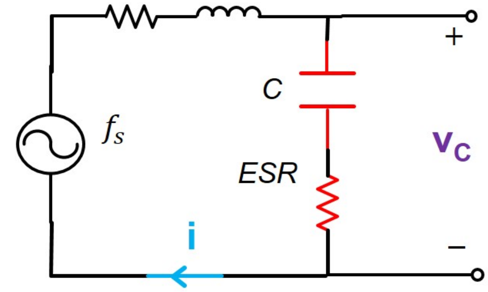

Fig. 7: Initial compensation circuit with high Q capacitor.

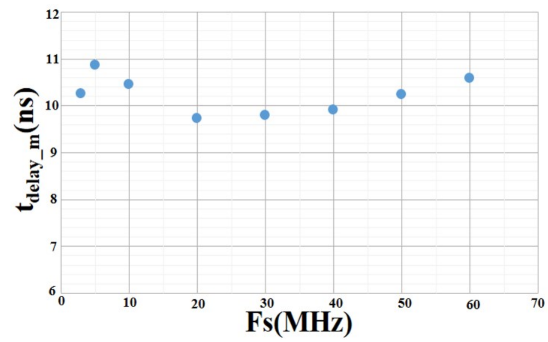

Fig. 8: Measured probe delay time vs frequency using high Q capacitor.

IV. Experimental Results

To validate the proposed method, the loss of three different type of core samples are measured under sinusoidal excitation. The excitation is supplied by a power amplifier 150A100C from Amplifier Research driven by a function generator, Tektronix AFG3102. The current probe TCP0030A and differential voltage probe TDP1000 are used to measure voltage and current. First, a 3F4 toroidal core from Ferrocube(TN14/10/2) is measured at 3MHz and 100°C temperature. At 3MHz, the measured delay time t_{delay_m} is 10.25ns and the tolerable delay time t_b is 15.7ns. Since t_{delay_m} is smaller than t_b, partial cancellation method can be performed directly without initial compensation.

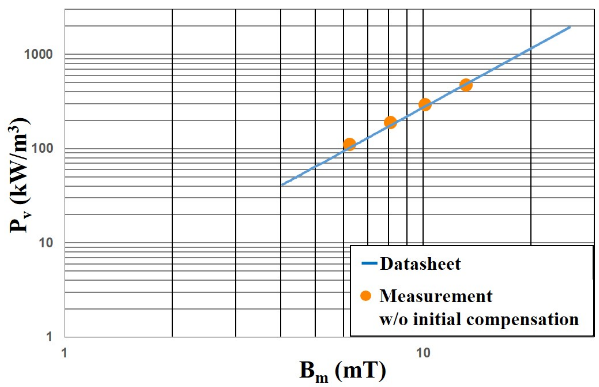

Fig. 9: Core loss of 3F4 at 3MHz, 100°C.

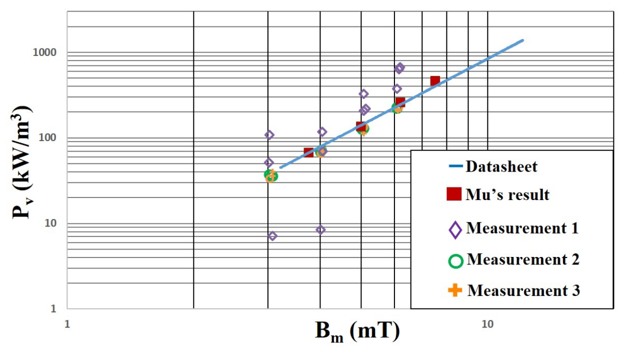

Fig. 10: Core loss of 4F1 at 10MHz, 100°C. Measurement 1:no compensation; Measurement 2:-10.45ns initial compensation; Measurement 3:-8ns initial compensation.

Fig.9 shows the measurement result. The measured loss without initial compensation matches very well with datasheet. Then a 4F1toroidal core from Ferrocube(TN21/19/3) is measured under 10MHz and 100°C. At 10MHz, t_{delay_m} is 10.45ns and t_b is 4.7ns. Therefore, -10.45ns should be added into current probe for initial compensation. The delay time from probe datasheet $t_{datasheet}$=8ns can also be used for compensation since t_{delay_m}-$t_{datasheet} < t_b$. For each condition, we measured the loss for 3 times as shown in Fig 10. Mu's measurement result in [11] is also provided for comparison. From Fig 10, the measured loss are different for each time and vary from datasheet and Mu's result without initial compensation. With initial compensation, the measured loss overlap with each other over 3 times and match well with datasheet and Mu's result. Finally, a toroidal core made by metal flake composite from TOKIN(TN14/10/1) is measured under 60MHz and 25°C. At 60MHz, t_{delay_m} is 10.58ns and t_b is 0.79ns. Fig 11 shows the measurement results. The measured loss with -10.58ns compensation is stable over 3 times. However, the measured loss with -8ns compensation varies each time. This is because t_{delay_m}-$t_{datasheet} > t_b$, which means the residual phase discrepancy is larger than the limit value using t_b=8ns for initial compensation, hence introducing

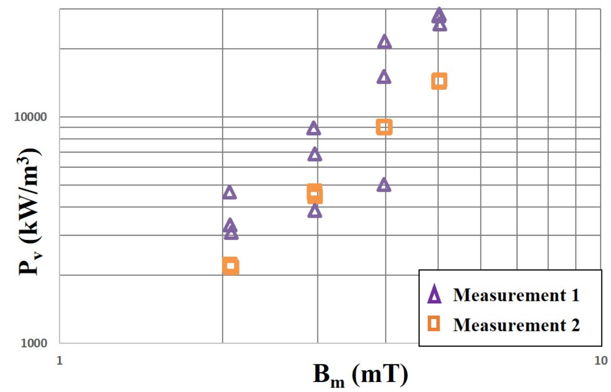

Fig. 11: Core loss of metal flake composite from TOKIN at 60MHz, 25°C. Measurement 1:-8ns compensation; Measurement 2:-10.58ns initial compensation.

loss error. Therefore, the fixed 8ns delay time provided by datasheet cannot be applied for compensation under higher frequency, which verifies previous analysis.

V. Conclusions

As a promising method for high frequency core loss measurement, partial cancellation method assumes phase discrepancy as a small value, which is not valid for high frequency. This paper first performs the error analysis under high frequency test condition. The result shows that large phase discrepancy will introduce non-negligible error and phase discrepancy need to be controlled in a small range to limit measured loss error. An initial compensation method is proposed to control phase discrepancy in a small range effectively by using a high Q capacitor. Finally, experiments verify the measurement accuracy of improved partial cancellation method.

Acknowledgement

This material is based upon work supported by the National Science Foundation under Award No. 1653156.

Disclaimer

Any opinions, findings, and conclusions or recommendations expressed in this material are those of the author(s) and do not necessarily reflect the views of the National Science Foundation.

References

[1] C. . Mathúna, N. Wang, S. Kulkarni, and S. Roy, "Review of Integrated Magnetics for Power Supply on Chip (PwrSoC)," *IEEE Transactions on Power Electronics*, vol. 27, pp. 4799–4816, Nov. 2012.

[2] F. C. Lee and Q. Li, "High-Frequency Integrated Point-of-Load Converters: Overview," *IEEE Transactions on Power Electronics*, vol. 28, pp. 4127–4136, Sept. 2013.

[3] F. Waldron, R. Foley, J. Slowey, A. N. Alderman, B. C. Narveson, and S. C. . Mathúna, "Technology Roadmapping for Power Supply in Package (PSiP) and Power Supply on Chip (PwrSoC)," *IEEE Transactions on Power Electronics*, vol. 28, pp. 4137–4145, Sept. 2013.

[4] Q. Li, Y. Dong, F. C. Lee, and D. J. Gilham, "High-Density Low-Profile Coupled Inductor Design for Integrated Point-of-Load Converters," *IEEE Transactions on Power Electronics*, vol. 28, pp. 547–554, Jan. 2013.

[5] Y. Su, Q. Li, and F. C. Lee, "Design and Evaluation of a High-Frequency LTCC Inductor Substrate for a Three-Dimensional Integrated DC/DC Converter," *IEEE Transactions on Power Electronics*, vol. 28, pp. 4354–4364, Sept. 2013.

[6] E. A. Burton, G. Schrom, F. Paillet, J. Douglas, W. J. Lambert, K. Radhakrishnan, and M. J. Hill, "FIVR — Fully integrated voltage regulators on 4th generation Intel® Core™ SoCs," in *2014 IEEE Applied Power Electronics Conference and Exposition - APEC 2014*, pp. 432–439, Mar. 2014.

[7] D. Hou, F. C. Lee, and Q. Li, "Very High Frequency IVR for Small Portable Electronics With High-Current Multiphase 3-D Integrated Magnetics," *IEEE Transactions on Power Electronics*, vol. 32, pp. 8705–8717, Nov. 2017.

[8] C. Xiao, G. Chen, and W. G. H. Odendaal, "Overview of Power Loss Measurement Techniques in Power Electronics Systems," *IEEE Transactions on Industry Applications*, vol. 43, pp. 657–664, May 2007.

[9] V. J. Thottuvelil, T. G. Wilson, and H. A. Owen, "High-frequency measurement techniques for magnetic cores," *IEEE Transactions on Power Electronics*, vol. 5, pp. 41–53, Jan. 1990.

[10] Y. Han, G. Cheung, A. Li, C. R. Sullivan, and D. J. Perreault, "Evaluation of Magnetic Materials for Very High Frequency Power Applications," *IEEE Transactions on Power Electronics*, vol. 27, pp. 425–435, Jan. 2012.

[11] M. Mu, Q. Li, D. J. Gilham, F. C. Lee, and K. D. T. Ngo, "New Core Loss Measurement Method for High-Frequency Magnetic Materials," *IEEE Transactions on Power Electronics*, vol. 29, pp. 4374–4381, Aug. 2014.

[12] D. Hou, M. Mu, F. C. Lee, and Q. Li, "New High-Frequency Core Loss Measurement Method With Partial Cancellation Concept," *IEEE Transactions on Power Electronics*, vol. 32, pp. 2987–2994, Apr. 2017.

[13] D. Hou, F. C. Lee, and Q. Li, "Magnetic characterization technique and materials comparison for very high frequency IVR," in *2016 IEEE Applied Power Electronics Conference and Exposition (APEC)*, pp. 657–662, Mar. 2016.

[14] F. D. Tan, J. L. Vollin, and S. M. Cuk, "A practical approach for magnetic core-loss characterization," *IEEE Transactions on Power Electronics*, vol. 10, pp. 124–130, Mar. 1995.

[15] "Tektronix tcp0030a datasheet." https://www.tek.com/datasheet/30-ac-dc-current-probe. [Online].

[16] "Tektronix tdp1000 datasheet." https://www.tek.com/sites/default/files/media/media/resources/51W_19997_6.pdf. [Online].

[17] "Abcs of probes primer." https://info.tek.com/www-abcs-of-probes-primer.html. [Online].